Available online at www.sciencedirect.com

ScienceDirect

Ceramics International 39 (2013) 9025–9031

CERAMICS INTERNATIONAL

www.elsevier.com/locate/ceramint

Hysteresis and vertical anisotropy of magnetoresistance in $La_{0.67}A_{0.33}MnO_z$ (A=Ca, Sr) polycrystalline films deposited on amorphous quartz substrates

Xiangrong Zhu[a,*], Zhigang Zhu[a], Cheng Chen[a], Honglie Shen[b], Koichi Tsukamoto[c], Takeshi Yanagisawa[c], Mamoru Okutomi[c], Noboru Higuchi[c]

[a]School of Urban Development and Environmental Engineering, Shanghai Second Polytechnic University, 2360 Jinhai Road, Shanghai 201209, PR China
[b]College of Materials Science & Technology, Nanjing University of Aeronautics & Astronautics, Nanjing 211100, PR China
[c]National Institute of Advanced Industrial Science and Technology, 1-1-4 Umezono, Tsukuba, Ibaraki 305-8568, Japan

Received 3 April 2013; received in revised form 26 April 2013; accepted 26 April 2013
Available online 9 May 2013

Abstract

Polycrystalline $La_{0.67}A_{0.33}MnO_z$ (A=Ca, Sr) thin films with [202] preferred orientation were synthesized on amorphous quartz substrates by means of metal organic deposition (MOD) technology. The Curie temperature (T_C) and metal–insulator transition temperature (T_p) are 172 K, 247 K and 227 K, 335 K for $La_{0.67}Ca_{0.33}MnO_z$ (LCMO) film and $La_{0.67}Sr_{0.33}MnO_z$ (LSMO) film, respectively. The hysteresis and vertical anisotropy behaviors of MR are exhibited by the films below T_C, which strongly relies on the magnetization process. The magnitude of these magnetotransport properties would decline with increasing temperature. The in-plane hysteric MR behaviors could be explained by multiple-domain model. For vertical anisotropy of MR, demagnetization effect plays an important role. Especially, compared to LCMO film, LSMO film still presents the above hysteretic MR effect and vertical anisotropic MR at RT due to its higher T_C.

Keywords: A. Hysteresis; B. Vertical anisotropic MR; C. LCMO film; D. LSMO film

1. Introduction

In the field of spintronics, $La_{0.67}A_{0.33}MnO_3$ (A=Ca, Sr) perovskite manganite materials, are still the research focus because of their high spin polarization and colossal magnetoresistance (CMR) properties [1–6], which will bring forth desirable applications on magnetic sensors, magnetic random access memory (MRAM), etc. The CMR properties of $La_{0.67}A_{0.33}MnO_3$ (A=Ca, Sr) manifest complexity. Firstly, the so-called low-field magnetoresistance (LFMR) effect has been widely reported in the materials. The spin-polarized intergrain tunneling or the spin-dependent scattering related to grain boundary or other structure defects is ascribed to LFMR [7–12]. Secondly, when the applied field is changed from positive direction to negative direction, the hysteresis of MR would occur. The magnetization process is decisive for the magnitude of MR hysteresis [13,14]. Thirdly, for the epitaxial film samples, in-plane anisotropic MR phenomena have been found [13–16]. When the angle between the magnetic field applied in the film plane and the current direction is transformed, the MR ratio will have a sinusoidal dependence on the angle. For the epitaxial films, magnetic crystalline anisotropy is an important fact responsible for the in-plane anisotropic MR [13]. Since the MR behavior is correlated with the angle between the magnetic field and current direction, it could be imagined that interesting magnetotransport phenomena would appear if the magnetic field was applied out of the film plane. In fact, the vertical anisotropy of MR has been reported on $La_{0.67}Ca_{0.33}MnO_3$ film synthesized by molecular beam epitaxy (MBE) or by pulsed laser deposition (PLD) when the field direction is vertical to the film plane [13,14].

*Corresponding author. Tel: +86 21 50215021x8537; fax: +86 21 50217725.
E-mail address: zhuxiangrong71@126.com (X. Zhu).

0272-8842/$ - see front matter © 2013 Elsevier Ltd and Techna Group S.r.l. All rights reserved.
http://dx.doi.org/10.1016/j.ceramint.2013.04.105

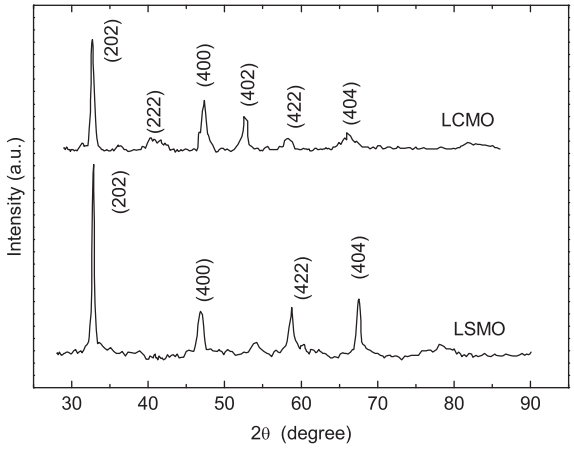

Fig. 1. The XRD spectra of LCMO film and LSMO film.

The study on the magnetotransport properties such as hysteresis and anisotropy of MR is significant for the application of CMR manganites. Hitherto, much more researches on magnetotransport properties are focused on epitaxial films synthesized on expensive single crystalline substrates such as (100) $LaAlO_3$ or (100) $SrTiO_3$ whose lattice constants are close to that of $La_{0.67}A_{0.33}MnO_3$ (A=Ca, Sr) [15,16]. However the polycrystalline films deposited on cheap substrates are also worth studying while considering the application cost. In this paper we reported the magnetotransport properties of polycrystalline $La_{0.67}A_{0.33}MnO_3$ (A=Ca, Sr) films synthesized on cheap amorphous quartz substrates by means of metal organic deposition (MOD) technology and also found the hysteresis and vertical anisotropy of MR in these films. The mechanism of these magnetotransport properties was discussed.

2. Experimental

As reported in a bit earlier paper [17], MOD is a simple and cheap technique for synthesizing manganite films for the substrates can be chosen randomly and the composition of the films can be adjusted conveniently. Here, the size of each amorphous quartz substrate for synthesizing $La_{0.67}A_{0.33}MnO_z$ (A=Ca, Sr) films was 1 cm × 1.5 cm. All substrates were in advance cleaned by ultrasonic cleaner and dried in an oven. For the MOD experiment, the starting solutions, $LaO_{1.5}$, $MnO_{1.5}$, SrO and CaO were purchased from Symetrix Corporation in Japan. Their molar concentrations were 0.1 −0.5 mol/l. According to the nominal composition of $La_{0.67}A_{0.33}MnO_z$ (A=Ca, Sr), the above starting solutions were mixed in such a way that the molar ratio of La:Sr (Ca): Mn was consistent with 2:1:3. Here, the oxygen composition is marked as z because the MOD annealing technique was conducted in air, which would result in the minor deviation of oxygen and non-stoichiometric oxygen. The mixed solutions were used as precursor solutions, spin-coated on the above clean substrates to form wet films. Then the wet films were baked in air at 473 K for 10 min. In order to increase the film thickness, the above process of preparing and baking gel films was repeated twice. After the baking, the gel films were annealed in air at 953 K−993 K for 50 min. After annealing all the samples were slowly cooled down to room temperature (RT) by shutting off the heat treatment system.

The samples were coded with LCMO and LSMO, corresponding to $La_{0.67}Ca_{0.33}MnO_z$ films and $La_{0.67}Sr_{0.33}MnO_z$ films, respectively. Rutherford backscattering spectra showed that the thickness of the films was about 100 nm−120 nm. The crystalline structure of the samples was determined by an X-ray diffractometer (XRD). The surface morphologies were observed by an atomic force microscope (AFM). The magnetotransport properties were measured by means of standard four-probe technique over a temperature range from 77 K to RT while the probe current was parallel to the longitudinal direction of the films. Finally, the magnetic properties of the samples were obtained from a SQUID magnetometer.

3. Results and discussion

The XRD spectra of LCMO and LSMO films are shown in Fig. 1. According to Fig. 1, both the samples manifest obvious polycrystalline perovskite structure. The strongest [202] peaks imply the [202] preferred orientation of the films. Moreover, for the two samples, the 2θ position of the strongest [202] peaks is very close, indicating that the difference of lattice constants between the LCMO and LSMO films is slight. Based on the pseudocubic unit cell, the lattice constants can be calculated as 0.382 nm and 0.386 nm for LCMO and LSMO, respectively, which are basically consistent with the results of the epitaxial films reported in other references [18–20].

Fig. 2 displays the 5 μm × 5 μm AFM images of the surface morphologies of LCMO and LSMO. It could be noticed that the surface morphologies of the two samples are similar. First, near round particles were grown smoothly and uniformly on the quartz substrates. The size of the particles ranges from 200 nm to 300 nm. At the same time, the structure of each film seems a bit porous, meaning the films are not dense and the grain boundaries are weakly linked. In addition, the surface root mean square (RMS) roughness is 7.5 nm and 8.2 nm for LCMO and LSMO, respectively, indicating that the average size of LSMO grains might be a bit larger than of LCMO grains.

The temperature dependences of normalized resistivity of LCMO and LSMO films under zero field are plotted in Fig. 3. Here the normalized resistivity is defined as ρ_T/ρ_{max}, where ρ_{max} is the maximum resistivity. Either LCMO film or LSMO film presents only one resistivity peak under zero field, corresponding to the typical metal–insulator transition. The data of metal−insulator transition peak temperature (T_p) are 172 K for LCMO and 227 K for LSMO. Usually for epitaxial CMR films, the T_p is always close to the Curie temperature (T_C), meeting with the double-exchange theory. For our samples, the T_C had been measured, namely 247 K for LCMO and 335 K for LSMO. Thus T_p of LCMO or LSMO is far lower than the corresponding T_C. According to our previous research [17], the great difference between T_p and T_C results from the porous structure defects of the samples, which could cause

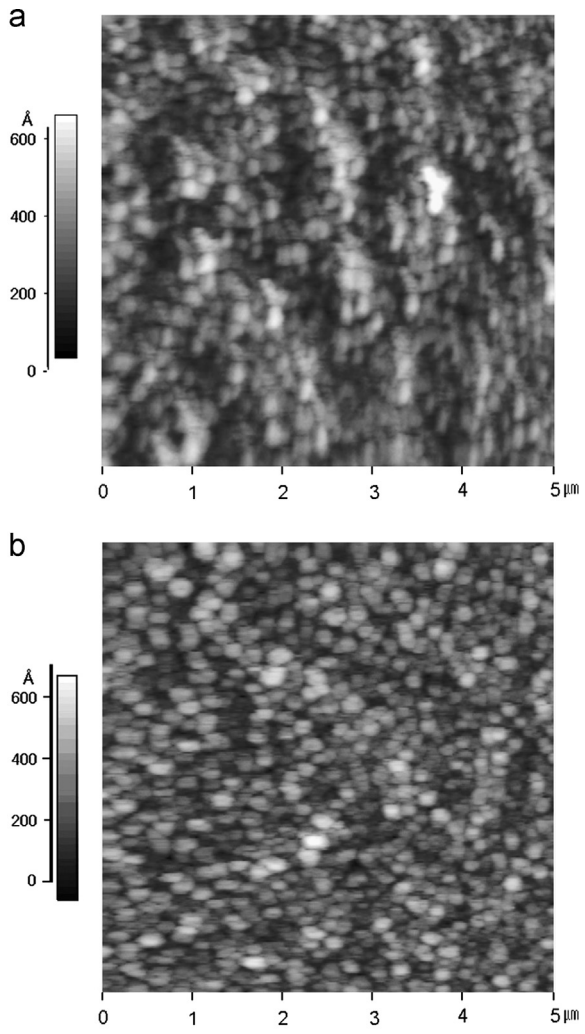

Fig. 2. The 5 μm × 5 μm AFM images of surface morphology of LCMO film (a) and LSMO film (b).

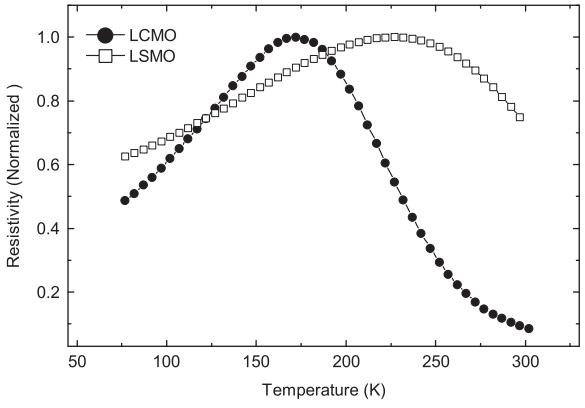

Fig. 3. Temperature dependences of normalized resistivity under zero field for LCMO film and LSMO film.

weak-linked grain boundaries and change of spin-dependent scattering properties.

The field dependences of normalized resistivity of LCMO and LSMO films were investigated at different temperatures, namely 77 K, T_p and RT (about 297 K), respectively. Here, T_p is 172 K for LCMO film and 227 K for LSMO film. The magnetic field was scanned from +10 kOe to −10 kOe and back. The direction of the field was adopted as two modes. One was that the field was parallel to the current in the film plane. The other was that the field was vertical to the film plane. Additionally, the magnetic hysteresis loops at 77 K and T_p were also measured. The results are displayed in Figs. 4 and 5. First, for both LCMO and LSMO films, at 77 K and T_p, while the field is parallel to the current in the film plane, the normalized resistivity $\rho_H/\rho_{(H=0)}$ presents hysteresis change within a certain field range. Beyond this range, the normalized resistivity changes linearly with the applied field. In the hysteresis zone, in the one hand, the maximum resistivity is not located at zero field but at a certain field, defined as switching field H_p. Thus, the MR partly manifests positive in the hysteresis zone. On the other hand, the low-field MR (LFMR) behavior is observed and sharp MR peak appears near H_p. Secondly, in the case of field parallel to film plane, the hysteresis loops at 77 K and T_p exhibit typical soft magnetism properties. Beyond 3 kOe field the magnetization would get saturated. Thirdly, while the field is applied vertical to the film plane at 77 K and T_p, vertical anisotropic MR behaviors appear. The LFMR is strongly suppressed and the MR peaks get blunt, showing upward-curving MR curves among the hysteric zones. Accordingly the hysteresis loops decline accompanied with smaller remnant magnetization and larger saturation field, which reveals the vertical anisotropy of magnetization. Finally, at RT, it could be noticed that CMR properties disappear for LCMO film. But for LSMO film, the properties of hysteresis and vertical anisotropy of MR remain at RT.

Considering the fact that ferromagnetism would disappear at RT for LCMO film, Fig. 6 only displays the hysteresis loops of LSMO film at RT with the field parallel and vertical to the film plane. Like the conditions at 77 K and 227 K, vertical anisotropy of magnetization is also shown at RT.

Table 1 lists the data of coercive field H_C, switching field H_p and maximum positive MR at 77 K and T_p for both LCMO and LSMO samples and those data at RT for LSMO film under the magnetic field parallel to the film plane. Here, the maximum positive MR is calculated as $[\rho_{(Hp)}-\rho_{(H=0)}]/\rho_{(H=0)} \times 100\%$, showing the magnitude of hysteresis. According to Table 1, whether for LCMO or for LSMO, the data of H_C, H_p and maximum positive MR decrease quickly with the temperature increasing from 77 K to T_p or RT temperature. Moreover, at same temperature, H_p is near H_C although H_p is always a bit larger than H_C. Under condition of field vertical to film plane, the data of coercive field H_C, switching field H_p and maximum positive MR at 77 K and T_p for both LCMO and LSMO samples and those data at RT for LSMO film are listed in Table 2. Just similar to the condition of field parallel to film plane, when the field is vertical to the film plane, the data of H_C, H_p also decrease quickly with the temperature increasing from 77 K to T_p or RT temperature. But the data of maximum positive MR become small and could almost be neglected at RT for LSMO film.

The results shown in Figs. 3 and 4, Tables 1 and 2 reveal the intimate correlation between the magnetotransport properties and magnetization process and this correlation manifests

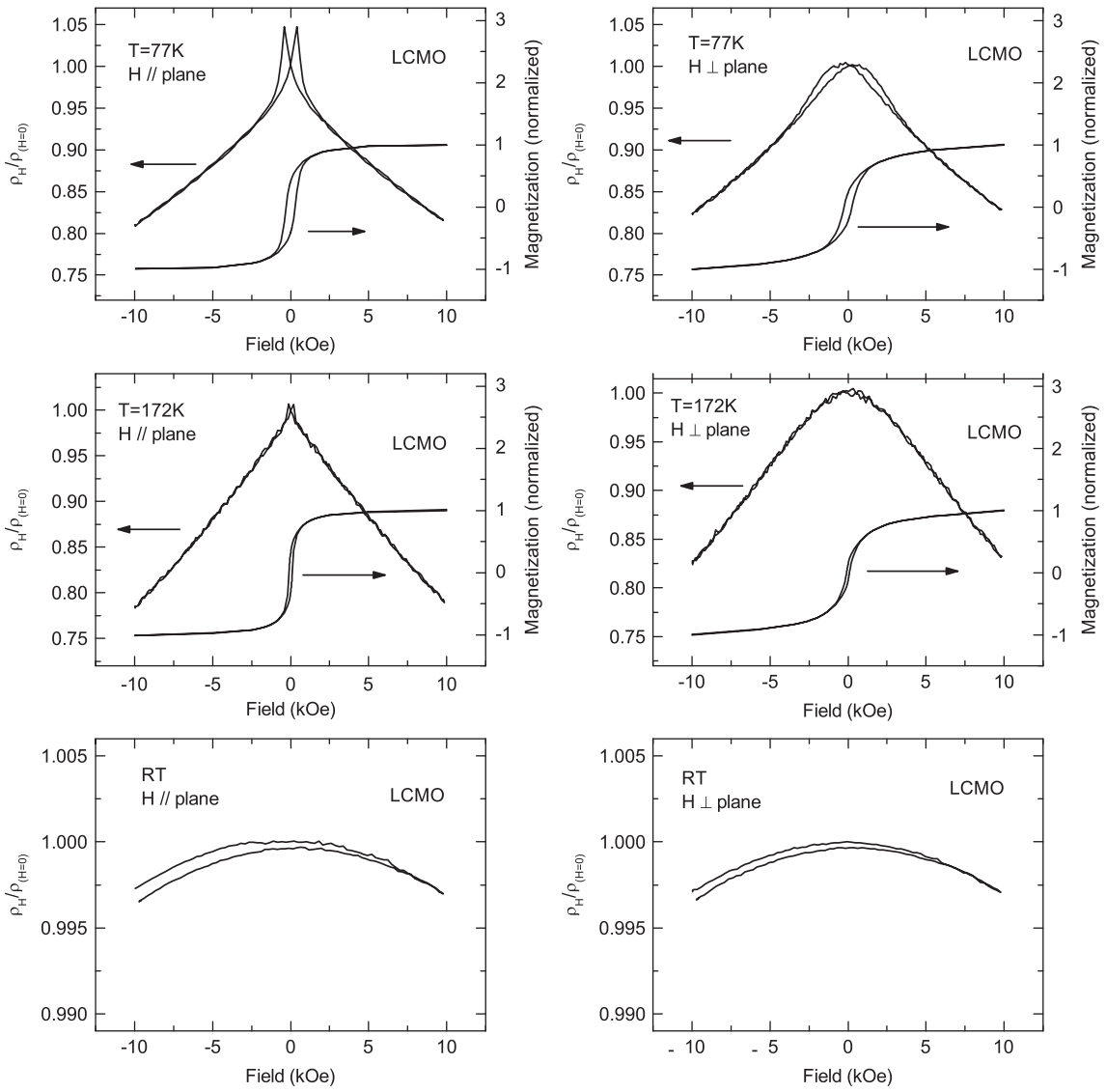

Fig. 4. Magnetic field dependences of normalized resistivity $\rho_H/\rho_{(H=0)}$ at 77 K, T_p (172 K) and RT and magnetic hysteresis loops at 77 K and T_p for LCMO film. The left column of this figure is corresponding to the condition of field parallel to the film plane and the right column is corresponding to the condition of field vertical to the film plane.

complex, which is determined by the structure characteristics of samples. The hysteric MR behaviors of our samples are basically similar to those of the epitaxial films [13,14]. Additionally, for epitaxial films, easy axes for magnetization plays important roles in-plane anisotropy MR [13–15]. O'Donnell once put forward a multiple-domain model to explain the hysteresis and in-plane anisotropy MR behaviors in epitaxial LCMO films [13]. At magnetic fields far greater than the switching field H_p, the sample is a single domain. At moderate fields near H_p, multiple domains parallel to the easy axes exist in varying abundance determined by applied field. Under the multiple-domain model, the magnetization reversal proceeds via motion of domain walls.

The resistivity of the sample is composed of three components, namely the resistivity of domains parallel to the applied field, the resistivity of antiparallel domains and the resistivity of perpendicular domains. Under different conditions of applied field, the data of the three components of resistivity would be correspondingly changed. Under field applied parallel to the film plane, as domain walls move, the MR deviates from linearity due to the growth of transverse (to the applied field) domains with higher or lower resistivity. The reversal of magnetization near H_C would lead to steep change of the resistivity. When the field is still parallel to film plane but vertical to current, the collapse into the aligned magnetic state can cause an increase or decrease in resistivity and then anisotropic MR. Detailed discussion about multiple-domain model could be seen in Ref. 13.

For our samples, although they are polycrystalline on amorphous quartz substrates, the similar in-plane hysteretic MR behaviors to those of epitaxial samples imply the existence of magnetocrystalline anisotropy in our samples, which might be related to the structural characteristics with [202] preferred orientation of the samples. Furthermore, the polycrystalline

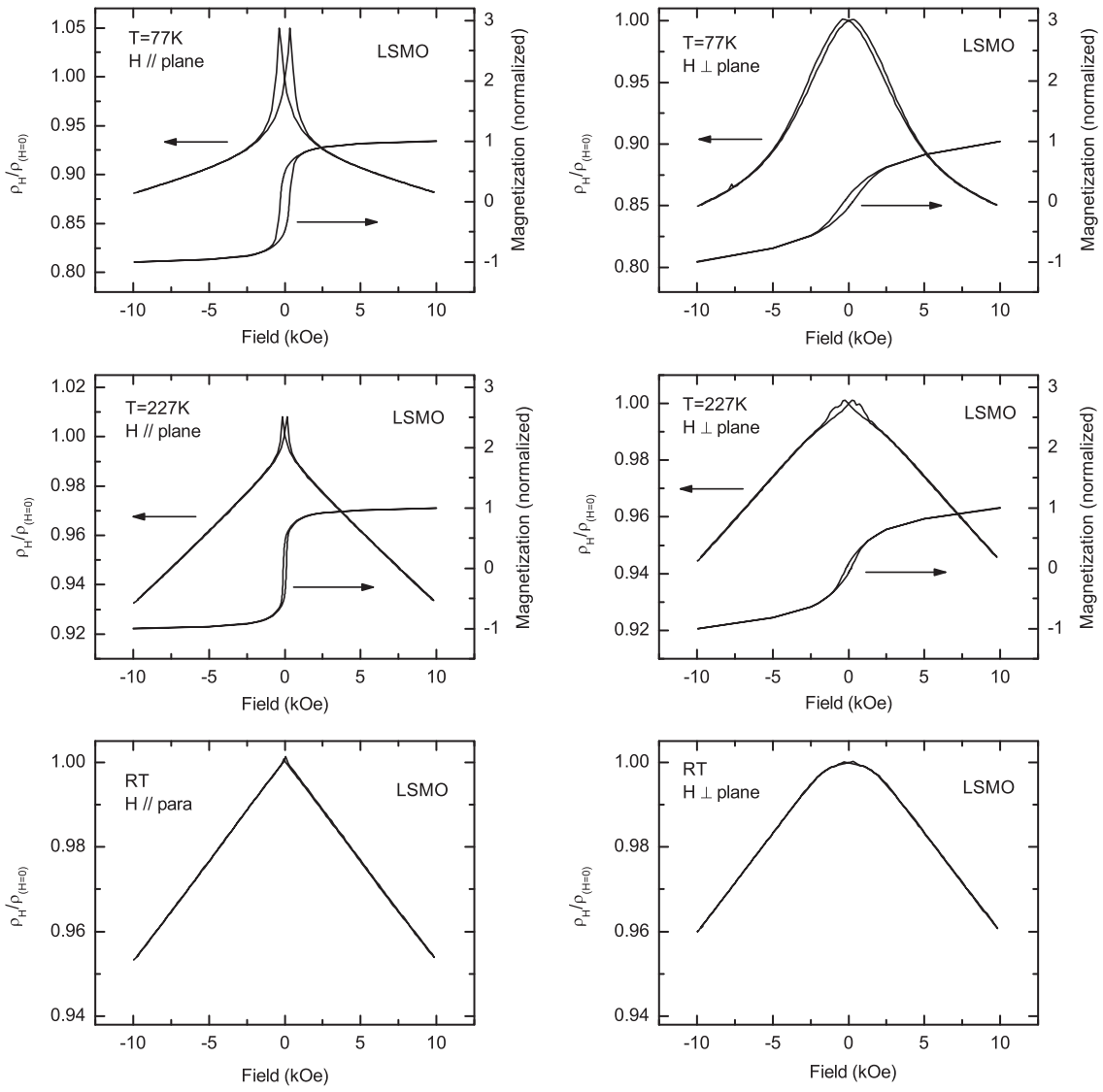

Fig. 5. Magnetic field dependences of normalized resistivity $\rho_H/\rho_{(H=0)}$ at 77 K, T_p (227 K) and RT and magnetic hysteresis loops at 77 K and T_p for LSMO film. The left column of this figure is corresponding to the condition of field parallel to the film plane and the right column is corresponding to the condition of field vertical to the film plane.

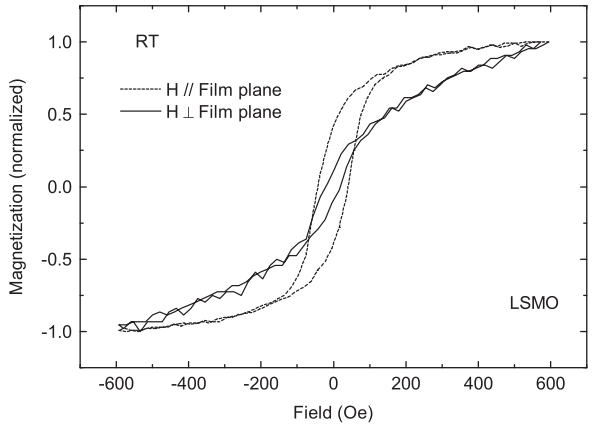

Fig. 6. Magnetic hysteresis loops of LSMO film at RT within ± 600 Oe field.

films could be regarded as the samples with multiple domains. Thus the multiple domain-model given by O'Donnell [13] might be well used to explain the in-plane hysteretic MR for our samples. However, this model might not be entirely suitable for analyzing the vertical anisotropy of MR of our samples. For the thin films the effect of demagnetizing field should be emphasized [21]. While the field is vertical to the film plane, the demagnetizing field direction is opposite to applied field, canceling the applied field as the magnetization begins to rotate out of the plane. Thus the hysteresis loops would decline and vertical anisotropy of magnetization occurs. Correlated with the spin–orbit interaction [22], the vertical magnetization would result in quadratic dependence of MR on applied field, namely the vertical anisotropic of MR, just like the results shown in Figs. 3 and 4.

Table 1
Data of coercive field H_C, switching field H_p and maximum positive MR at 77 K and T_p for both LCMO and LSMO samples and those data at RT for LSMO film under the magnetic field parallel to the film plane.

	H_C (Oe)			H_p (Oe)			Maximum positive MR		
LCMO (H//plane)	77 K	172 K		77 K	172 K		77 K	172 K	
	300	115		340	120		4.7%	0.7%	
LSMO (H//plane)	77 K	227 K	RT	77 K	227 K	RT	77 K	227 K	RT
	310	110	40	350	165	50	5%	0.8%	0.1%

Table 2
Data of coercive field H_C, switching field H_p and maximum positive MR at 77 K and T_p for both LCMO and LSMO samples and those data at RT for LSMO film under the magnetic field vertical to the film plane.

	H_C (Oe)			H_p (Oe)			Maximum positive MR		
LCMO (H⊥film)	77 K	172 K		77 K	172 K		77 K	172 K	
	280	100		280	110		0.4%	0.2%	
LSMO (H⊥film)	77 K	227 K	RT	77 K	227 K	RT	77 K	227 K	RT
	300	120	20	380	180	50	0.1%	0.1%	0.04%

Since the magnetotransport properties entirely rely on the magnetization process, the fact that the effects of hysteretic MR and anisotropy MR would decline with increasing temperature and disappear at temperature above the Curie temperature T_C could be understood. As demonstrated by Fig. 5, LSMO keeps substantial MR properties at RT. Thus LSMO film shows more desirable application than LCMO film.

4. Conclusion

In summary, $La_{0.67}A_{0.33}MnO_3$ (A = Ca, Sr) thin films were synthesized on amorphous quartz substrates by means of MOD. The XRD spectra show that all the samples are polycrystalline with [202] preferred orientation. The hysteresis and vertical anisotropy of MR are exhibited by the films below Curie temperature T_C, which are strongly correlated with the magnetization process. The in-plane hysteric MR behaviors could be explained by multiple-domain model. But for vertical anisotropy of MR, demagnetization effect should be considered. The effects of hysteretic MR and anisotropy MR would decline with increasing temperature and disappear at temperature above T_C. Because the LSMO film exhibits higher T_c above RT, it still retains certain CMR properties near RT and thus presents more desirable application prospects than LCMO film.

Acknowledgments

The authors would like to acknowledge the financial supports from the Open Fund of State Key Laboratory of Functional Materials for Informatics, Shanghai Institute of Microsystem and Information Technology, Chinese Academy of Sciences, the Program for Professor of Special Appointment (Eastern Scholar) at Shanghai Institutions of Higher Learning and the University Grant from Shanghai Second Polytechnic University (A30XK121101).

References

[1] A. Mraković, J. Blanuša, D. Primc, Ma. Perović, Z. Jagličić, V. Kusigerski, V. Spasojević, Modified self-propagating high-temperature synthesis of nanosized $La_{0.7}Ca_{0.3}MnO_3$, Ceramics International 39 (2013) 3771–3777.
[2] V.S. Kolat, H. Gencer, M. Gunes, S. Atalay, Effect of B-doping on the structural, magnetotransport and magnetocaloric properties of $La_{0.67}Ca_{0.33}MnO_3$ compounds, Materials Science and Engineering B 140 (2007) 212–217.
[3] C. Moreno, C. Munuera, S. Valencia, F. Kronast, X. Obradors, C. Ocal, Reversible resistive switching and multilevel recording in $La_{0.7}Sr_{0.3}MnO_3$ thin films for low cost nonvolatile memories, Nano Letters 10 (2010) 3828–3835.
[4] D. Bahadur, D. Das, Properties of CMR composites, Proceedings of the Indian Academy of Sciences: Chemical Sciences 115 (5–6) (2003) 587–606.
[5] L.W. Martin, Y.-H. Chu, R. Ramesh, Advances in the growth and characterization of magnetic, ferroelectric, and multiferroic oxide thin films, Materials Science and Engineering R 68 (2010) 89–133.
[6] M. Shiraishi, T. Ikoma, Molecular spintronics, Physica E 43 (2011) 1295–1317.
[7] L.W. Lei, Z.Y. Fu, J.Y. Zhang, Hao Wang, K. Niihara, Low field magnetoresistance of $La_{0.7}Ca_{0.3}MnO_3$ ceramics fabricated by fast sintering process, Journal of Alloys and Compounds 530 (2012) 164–168.
[8] S.P. Isaac, N.D. Mathur, J.E. Evetts, M.G. Blamire, Magnetoresistance of artificial $La_{0.7}Sr_{0.3}MnO_3$ grain boundaries as a function of misorientation angle, Applied Physics Letters 72 (1998) 2038–2040.
[9] G.L. Yuan, J.-M. Liu, H.L.W. Chan, C.L. Choy, C.K. Ong, Z.G. Liu, Y.W. Du, Low-field magnetoresistance in oxygen-deficient $La_{0.5}Sr_{0.5}MnO_3$ thin films as approached by spin-polarized tunneling model, Materials Letters 53 (2002) 76–82.
[10] J.Y. Gu, S.B. Ogale, M. Rajeswari, T. Venkatesan, R. Ramesh, V. Radmilovic, U. Dahmen, G. Thomas, T.W. Noh, In-plane grain boundary effects on the magnetotransport properties of $La_{0.7}Sr_{0.3}MnO_{3-\delta}$, Applied Physics Letters 72 (1998) 1113–1115.
[11] X.L. Wang, S.X. Dou, H.K. Liu, M. Ionescu, B. Zeimetz, Large low-field magnetoresistance over a wide temperature range induced by weak-link grain boundaries in $La_{0.7}Ca_{0.3}MnO_3$, Applied Physics Letters 73 (1998) 396–398.
[12] H.Y. Hwang, S.-W. Cheong, N.P. Ong, B. Batlogg, Spin-polarized intergrain tunneling in $La_{2/3}Sr_{1/3}MnO_3$, Physical Review Letters 77 (1996) 2041–2044.

[13] J. O'Donnell, M. Onellion, M.S. Rzchowski, Low-field magnetoresistance in tetragonal $La_{1-x}Ca_xMnO_3$ films, Physical Review B 55 (1997) 5873–5879.

[14] C. Srinitiwarawong, M. Ziese, Magnetoresistance of mechanically induced grain boundaries in $La_{0.7}Ca_{0.3}MnO_3$ films, Applied Physics Letters 73 (1998) 1140–1142.

[15] Soumen Mandal, R.C. Budhani, Magnetization depinning transition, anisotropic magnetoresistance and inplane anisotropy in two polytypes of $La_{2/3}Sr_{1/3}MnO_3$ epitaxial films, Journal of Magnetism and Magnetic Materials 320 (2008) 3323–3333.

[16] K. Zhao, L. Zhang, H.K. Wong, Anisotropic magnetoresistance in $La_{0.67}Ca_{0.33}MnO_3/YBa_2Cu_4O_8/La_{0.67}Ca_{0.33}MnO_3$ trilayer films, Thin Solid Films 471 (2005) 287–292.

[17] X.R. Zhu, H.L. Shen, Z.X. Tang, K. Tsukamoto, T. Yanagisawa, M. Okutomi, N. Higuchi, Characterization of $La_{0.67}Sr_{0.33}MnO_z$ thin films synthesized by metal-organic decomposition on different substrates, Ceramics International 38 (2012) 6405–6410.

[18] Y.X. Han, W.B. Wu, G.S. Jiang, C.F. Zhu, In-plane ordered grain boundaries inducing enhanced magnetoresistance in epitaxial manganite films, Applied Surface Science 258 (2012) 7245–7249.

[19] M. Španková, Š. Chromik, I. Vávra, K. Sedláčková, P. Lobotka, S. Lucas, S. Stanček, Epitaxial LSMO films grown on MgO single crystalline substrates, Applied Surface Science 253 (2007) 7599–7603.

[20] Z. Yang, L. Sun, C. Ke, X. Chen, W. Zhu, O. Tan, Growth and structure properties of $La_{1-x}Sr_xMnO_{3-\sigma}$ ($x=0.2$, 0.3, 0.45) thin film grown on $SrTiO_3$ (0 0 1) single-crystal substrate by laser molecular beam epitaxy, Journal of Crystal Growth 311 (2009) 3289–3294.

[21] J.N. Eckstein, I. Bozovic, J. O'Donnell, M. Onellion, M.S. Rzchowski, Anisotropic magnetoresistance in tetragonal $La_{1-x}Ca_xMnO_\delta$ thin films, Applied Physics Letters 69 (1996) 1312–1314.

[22] A.P. Malozemoff, Anisotropic magnetoresistance of amorphous and concentrated polycrystalline iron alloys, Physical Review B 32 (1985) 6080–6083.